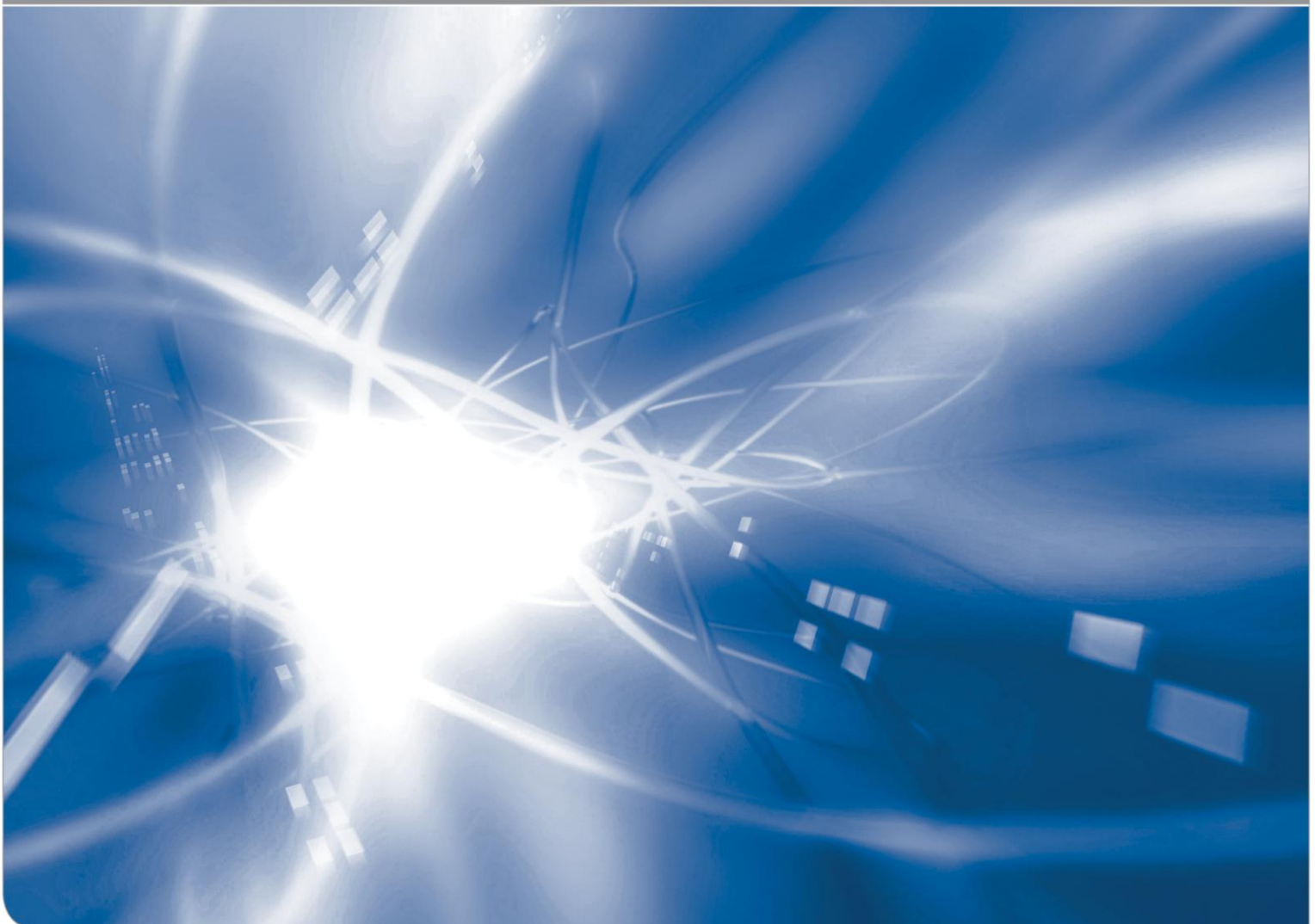


# Production of Vector Mesons by Photonuclear Interactions in the Program CORSIKA

by Dieter Heck<sup>1</sup>

KIT SCIENTIFIC WORKING PAPERS 6



<sup>1</sup> Institute for Nuclear Physics, Karlsruhe Institute of Technology (KIT)

### **Impressum**

Karlsruher Institut für Technologie (KIT)  
www.kit.edu



Diese Veröffentlichung ist im Internet unter folgender Creative Commons-Lizenz  
publiziert: <http://creativecommons.org/licenses/by-nc-nd/3.0/de>

2013

ISSN: 2194-1629

# Abstract

## **Production of Vector Mesons by Photo-Nuclear Interactions in the Program CORSIKA**

This report describes the production of vector mesons by photonuclear interactions in the air shower simulation program CORSIKA. These vector mesons  $\rho^0$  and  $\omega$  are produced also at the highest  $\gamma$ -energies and decay to only two charged pions (for  $\omega$  two charged and one neutral pion), which in turn by decay may lead to muons in the TeV-energy range. Details of the used parameterizations for the production process are given.

# Zusammenfassung

## **Produktion von Vektor-Mesonen durch photonukleare Wechselwirkungen im Programm CORSIKA**

Dieser Bericht beschreibt die Produktion von Vektormesonen durch photonukleare Wechselwirkungen in dem Luftschauer-Simulationsprogramm CORSIKA. Diese Vektormesonen  $\rho^0$  und  $\omega$  werden auch bei den höchsten  $\gamma$ -Energien produziert und zerfallen in nur zwei geladene Pionen (für  $\omega$  zwei geladene und ein neutrales Pion), die ihrerseits durch Zerfall zu Myonen im TeV-Energiebereich führen können. Details der benutzten Parametrisierungen für den Produktionsprozess werden angegeben.



## Contents

<b>1</b>	<b>Introduction</b>	<b>1</b>
<b>2</b>	<b>Cross-Section Data</b>	<b>2</b>
2.1	Parameterizations of total gamma-air cross-section . . . . .	2
2.2	Vector meson production at C, N, and O . . . . .	3
<b>3</b>	<b>Vector Meson Fraction of Photonuclear Interaction</b>	<b>5</b>
<b>4</b>	<b>Decay of Vector Mesons</b>	<b>6</b>
<b>5</b>	<b>Higher Mass Vector Mesons</b>	<b>7</b>
	<b>References</b>	<b>9</b>



# 1 Introduction

In the generalized vector dominance model [1, 2] a  $\gamma$ -ray is assumed to fluctuate into a quark-antiquark pair. Due to the interaction this off-mass shell pair is moved to the mass shell of a vector meson (VM) or a diffractively excited state of it. If a single VM is produced then this particle carries the quantum numbers of the incoming photon. In other words, the quark pair forms a  $(q\bar{q})^{J=1}$  bound state of a neutral VM which subsequently interacts by elastic scattering off a nucleon. Predominantly the VMs  $\rho^0$  and  $\omega$  have to be considered. The production of higher-mass neutral VMs is strongly suppressed as with increasing quark mass the probability to fluctuate into a  $s\bar{s}$ -pair leading to a  $\phi$ -meson or into a  $c\bar{c}$ -pair leading to a  $J/\psi$ -meson decreases.

With extremely short lifetimes the VMs decay into two charged pions ( $\rho^0$ ) resp. three pions ( $\omega$ ) which by the Lorentz-boost are emitted in the very forward direction of the incoming  $\gamma$ -ray:

$$\gamma + N \rightarrow \rho^0 + N \rightarrow \pi^+ + \pi^- + N$$

$$\gamma + N \rightarrow \omega + N \rightarrow \pi^+ + \pi^- + \pi^0 + N$$

Thus the  $\gamma$ -ray energy is distributed only onto very few charged pions.

In the higher atmosphere above some ten km where the air density is low the pion decay dominates over the pion interaction and energetic muons (and neutrinos) will emerge and carry away a large fraction of the primary  $\gamma$ -ray. This underlines the importance of the VM production process for muon generation in the development of cosmic ray air showers and therefore the VM production by  $\gamma$ -rays is implemented in the air shower simulation program CORSIKA [3].

## 2 Cross-Section Data

In CORSIKA the interactions of  $\gamma$ -rays are treated by the custom-made routines of the EGS4-package [4]. The  $\gamma$ -rays may initiate different processes and their branching ratios are defined by the ratios of the cross-sections. The total inelastic  $\gamma$ -ray cross-section (defining the mean free path to the next interaction) and the branching ratios leading to the different interaction processes are tabulated in the EGSDAT data files which are read in when starting the EGS4-package.

### 2.1 Parameterizations of total gamma-air cross-section

The hadronic interaction processes of  $\gamma$ -rays may happen at energies above the pion production threshold of  $E_{\gamma\text{lab}} > 0.1482$  GeV. At  $\gamma$ -energies below  $E_{\gamma\text{cm}} \leq 19.39$  GeV (equivalent  $E_{\gamma\text{lab}} \leq 200$  GeV) the photonuclear cross-section is described by a continuous distribution [5]

$$\sigma_{\gamma p} = (73.7 s^{0.073} + 191.7 s^{-0.602}) \sqrt{1 - s_0/s} \quad (1)$$

where  $s$  is the squared cm-energy (in  $\text{GeV}^2$ ) and  $s_0$  is the pion production threshold energy with  $\sqrt{s_0} = 1.0761$  GeV. The resulting cross-section  $\sigma_{\gamma p}$  is given in  $\mu\text{b}$ . The root on the rhs. of Eq. 1 cuts down the cross-section at the threshold energy. Superimposed on this continuous distribution are three resonances at squared cm-energies of 1.464, 2.220, and 2.789  $\text{GeV}^2$  with width parameters of 0.12705, 0.18774, and 0.19372  $\text{GeV}^2$  and amplitude parameters of 54.2, 23.2, and 11.2  $\mu\text{b}/\text{GeV}^2$ , respectively. How well the experimental data points are described by this parameterization of the resonance structure of the  $\gamma$ -p cross-section is demonstrated in Fig. 7.1 of Ref. [3].

Above  $E_{\gamma\text{cm}} > 19.39$  GeV the parameterization of Ref. [6, 7] is used (again  $\sigma_{\gamma p}$  in  $\mu\text{b}$ ):

$$\sigma_{\gamma p} = 59.3 s^{0.093} + 120.2 s^{-0.358} \quad (2)$$

The two slope parameters in the exponents and the amplitude factors are results of global fits [6] which include  $pp$  and  $p\bar{p}$  measurements and use corresponding ratios of the real-to-imaginary part of the forward scattering amplitudes. This guarantees a reliable extrapolation of Eq. 2 to highest energies. The smooth transition of the cross-section  $\sigma_{\gamma p}$  at  $E_{\gamma\text{cm}} = 19.39$  GeV between the two energy ranges of Eq. 1 and Eq. 2, respectively, has been checked.

For a target nucleus of mass number  $A$  the total inelastic  $\gamma$ - $A$  cross-section is derived from the  $\gamma$ -p cross-section by scaling with  $A^{0.91}$  according Ref. [5, 8]. For the three constituents of air with Nitrogen ( $A = 14$ , 75.528%), Oxygen ( $A = 16$ , 23.166%), and Argon ( $A = 40$ , 1.282%) we scale the cross-section for each

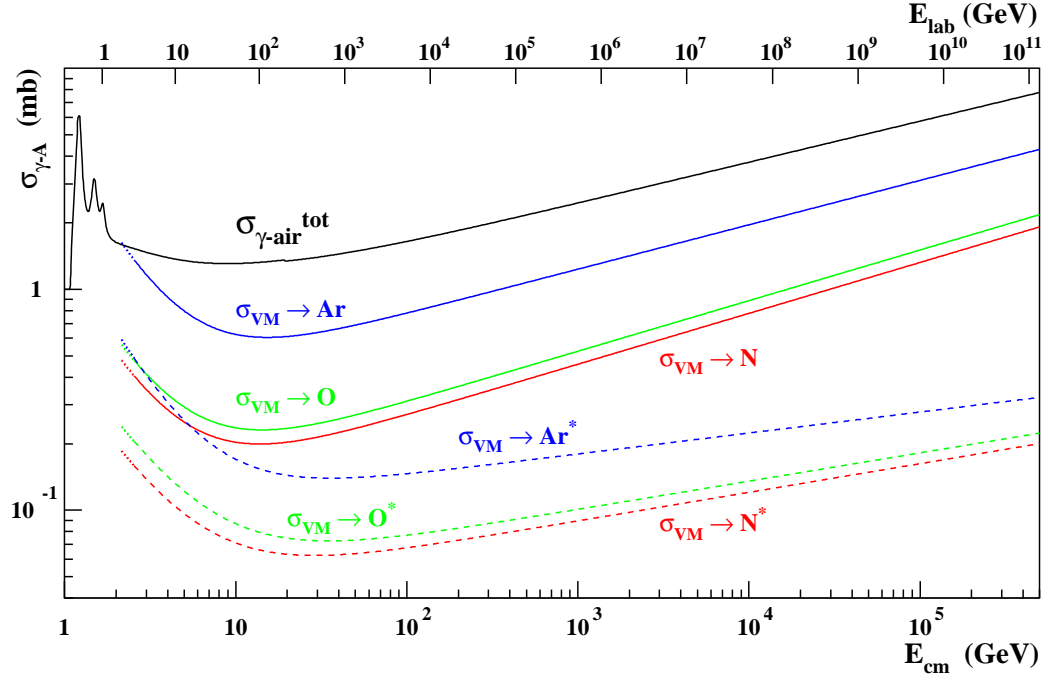


Figure 1: Total photonuclear cross-section of air (black solid line) and VM production cross-sections of the different constituents of air leading to ground state (solid coloured lines) or excited state (dashed coloured lines) target nuclei are plotted as function of the cm-energy in the  $\gamma$ -nucleon system.

component and form the weighted sum from the three individual elemental cross-sections.

The resulting total inelastic  $\gamma$ -air cross-section is shown in Fig. 1 as function of the cm-energy in the  $\gamma$ -nucleon system.

## 2.2 Vector meson production at C, N, and O

The cross-section for the photoproduction of VMs is parameterized [9, 10] in the form

$$\sigma(E_{\text{cm}}) = a \cdot E_{\text{cm}}^{\delta} + b \cdot E_{\text{cm}}^{-\epsilon} \quad (3)$$

where the energy  $E$  is used in the cm-system (in GeV) of the  $\gamma$ -nucleon system and the resulting cross-section is given in mb. The parameters  $a$ ,  $\delta$ ,  $b$ , and  $\epsilon$  used in Eq. 3 for the individual components of air are listed in Table 1 for target nuclei remaining in the ground state or in an excited state.

Table 1: Cross-section parameters [9] according Eq. 3 for VM production at the constituents of air with target nuclei remaining in ground state and excited state (marked by \*) (after [10]).

Reaction	a	b	$\delta$	$\epsilon$
$\gamma + N \rightarrow VM + N$	0.0932 $\pm 0.0062$	1.044 $\pm 0.509$	0.2304 $\pm 0.0091$	1.369 $\pm 0.319$
$\gamma + N \rightarrow VM + N^*$	0.0365 $\pm 0.0023$	0.372 $\pm 0.105$	0.1297 $\pm 0.0084$	1.230 $\pm 0.182$
$\gamma + O \rightarrow VM + O$	0.1076 $\pm 0.0074$	1.222 $\pm 0.591$	0.2292 $\pm 0.0094$	1.358 $\pm 0.316$
$\gamma + O \rightarrow VM + O^*$	0.0417 $\pm 0.0050$	0.482 $\pm 0.222$	0.1280 $\pm 0.0160$	1.191 $\pm 0.291$
$\gamma + Ar \rightarrow VM + Ar$	0.3074 $\pm 0.0211$	3.835 $\pm 1.988$	0.2010 $\pm 0.0094$	1.449 $\pm 0.334$
$\gamma + Ar \rightarrow VM + Ar^*$	0.0931 $\pm 0.0144$	1.475 $\pm 1.148$	0.0950 $\pm 0.0211$	1.435 $\pm 0.485$

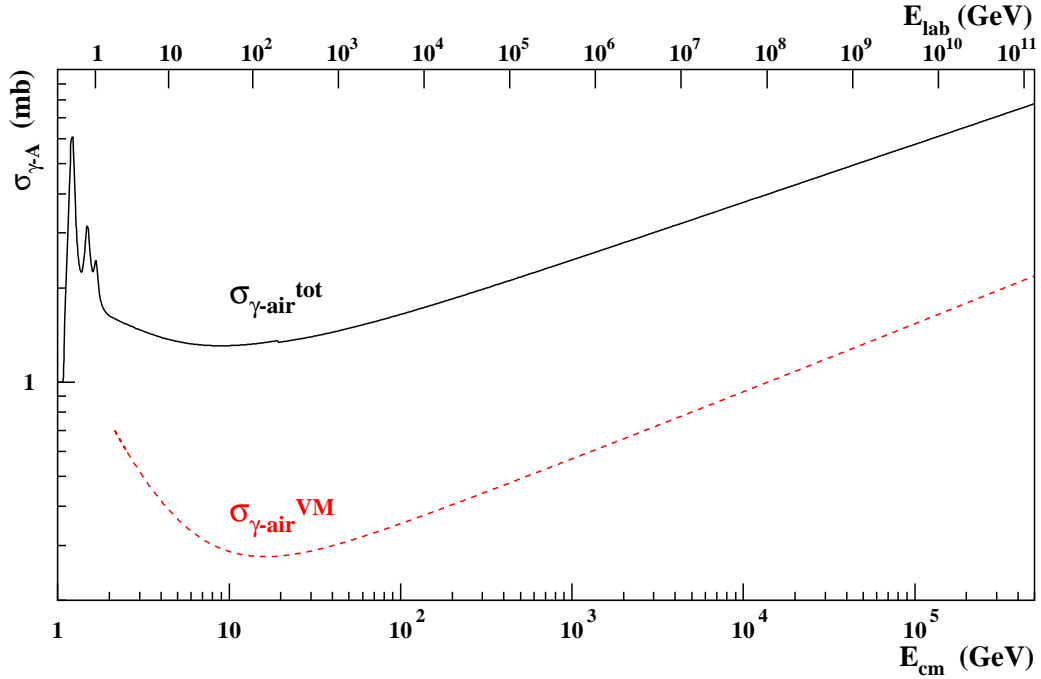


Figure 2: The total photonuclear cross-section of air (black solid line) and the VM production cross-section of air (dashed red line) including contributions leading to ground states and excited states of the air constituents is plotted as function of the cm-energy in the  $\gamma$ -nucleon system.

The resulting VM production cross-sections are plotted in Fig. 1. In these parameterizations the contribution ratio of  $\rho^0$  and  $\omega$  mesons is assumed [11] to be 9 : 1, while the production of  $\phi$  or heavier VMs is neglected, see also Sect. 5.

Summing up the weighted contributions of all components of air we arrive at the total  $\gamma$ -air VM production cross-section which is shown in Fig. 2.

### 3 Vector Meson Fraction of Photonuclear Interaction

From the two functions plotted in Fig. 2 we form the quotient  $\sigma_{\gamma\text{air}}^{\text{VM}} / \sigma_{\gamma\text{air}}^{\text{tot}}$  which is displayed in Fig. 3. Taking typically two points per  $E_{\text{cm}}$ -decade and adding some more points around  $E_{\text{cm}} \approx 10$  GeV where the VM fraction shows a strong bending of the curve we fit to the 15 selected points the function of Eq. 4 which is of the form of Eq. 3.

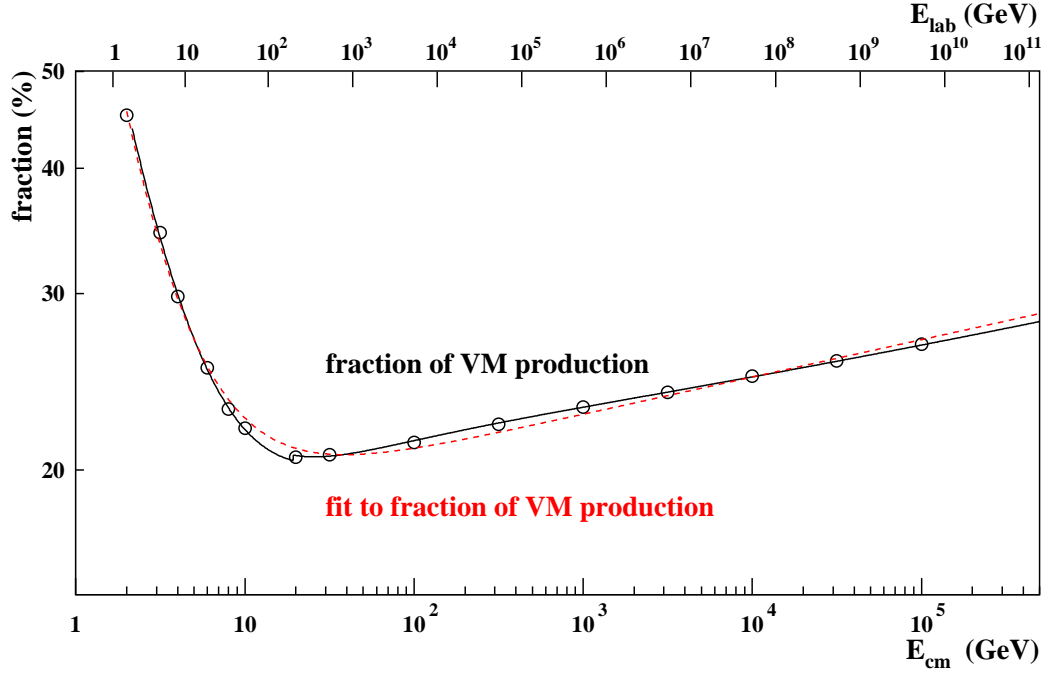


Figure 3: Fraction of VM production (solid line) calculated from the quotient  $\sigma_{\gamma\text{air}}^{\text{VM}} / \sigma_{\gamma\text{air}}^{\text{tot}}$  as function of the cm-energy (in the  $\gamma$ -nucleon system). 15 points of this distribution have been selected (open circles) and the function (dashed line) of Eq. 4 is fitted to them.

The final parameters of the fit result in the VM fraction as function of the cm-energy in the  $\gamma$ -nucleon system to

$$\text{fraction}_{\text{VM}} = 0.17560 \cdot E_{\text{cm}}^{0.037303} + 0.68008 \cdot E_{\text{cm}}^{-1.3021} . \quad (4)$$

This function follows rather closely the selected points, see Fig. 3.

## 4 Decay of Vector Mesons

The decay modes of the different VMs are listed in Tabel 2. In CORSIKA in all decays only modes with a branching ratio  $\geq 1$  % are respected. All those modes are given for the  $\rho^0$ ,  $\omega$  and  $\phi$ -mesons. For the  $\psi$ -meson only the mode leading to a high-energy  $\mu^+\mu^-$ -pair is shown.

Table 2: Lifetime and decay modes of vector mesons with branching ratios  $\geq 1$  % (after [7]). For the  $\psi$ -meson only the interesting  $\mu^+\mu^-$ -decay mode leading to high-energy muons is listed.

vector meson	lifetime (s)	decay mode	branching ratio
$\rho^0$	$4.50 \cdot 10^{-24}$	$\pi^+ \pi^-$	$\approx 100$ %
$\omega$	$7.75 \cdot 10^{-23}$	$\pi^+ \pi^- \pi^0$	89.2 %
		$\pi^0 \gamma$	8.28 %
		$\pi^+ \pi^-$	1.53 %
$\phi$	$1.55 \cdot 10^{-22}$	$K^+ K^-$	48.9 %
		$K_L^0 K_S^0$	34.2 %
		$\rho \pi$ $\pi^+ \pi^- \pi^0$	} 15.32 %
		$\eta \gamma$	1.309 %
$\psi$	$7.01 \cdot 10^{-21}$	...	...
		$\mu^+ \mu^-$	5.93 %
		...	...

The VMs are produced preferentially by the transverse polarization of the incoming  $\gamma$ -ray. Therefore the  $\pi^+\pi^-$ -pair from the two-body decay of the VMs is emitted preferentially in transverse direction with the characteristic dipole angular distribution  $I \propto \sin^2 \theta_{\text{cm}}$  with  $\theta_{\text{cm}}$  denoting the polar angle relative to the VM direction in the cm-system. This is considered in CORSIKA for the decaying  $\rho^0$ -meson using the experimentally found parameter of the ZEUS Collaboration [12]

$$I(\theta_{\text{cm}}) \propto (1 - 0.8836 \cdot \cos^2 \theta_{\text{cm}})$$

The three-body decay of the  $\omega$ -meson is treated with correct kinematics, but without any angular preference. A homogeneous distribution in the corresponding Dalitz plot is assumed. Also for the two other respected two-body decays of the  $\omega$ -meson no angular alignments of the decay directions are assumed.

The lifetime of the VMs is too short to respect any transport between VM creation and decay. Therefore in the CORSIKA program the VM production position is taken as vertex point of the decay.

## 5 Higher Mass Vector Mesons

In the SU(6) theory one assumes the photon to couple to the charge of the participating quarks which determines [13] the photoproduction cross-section ratio to

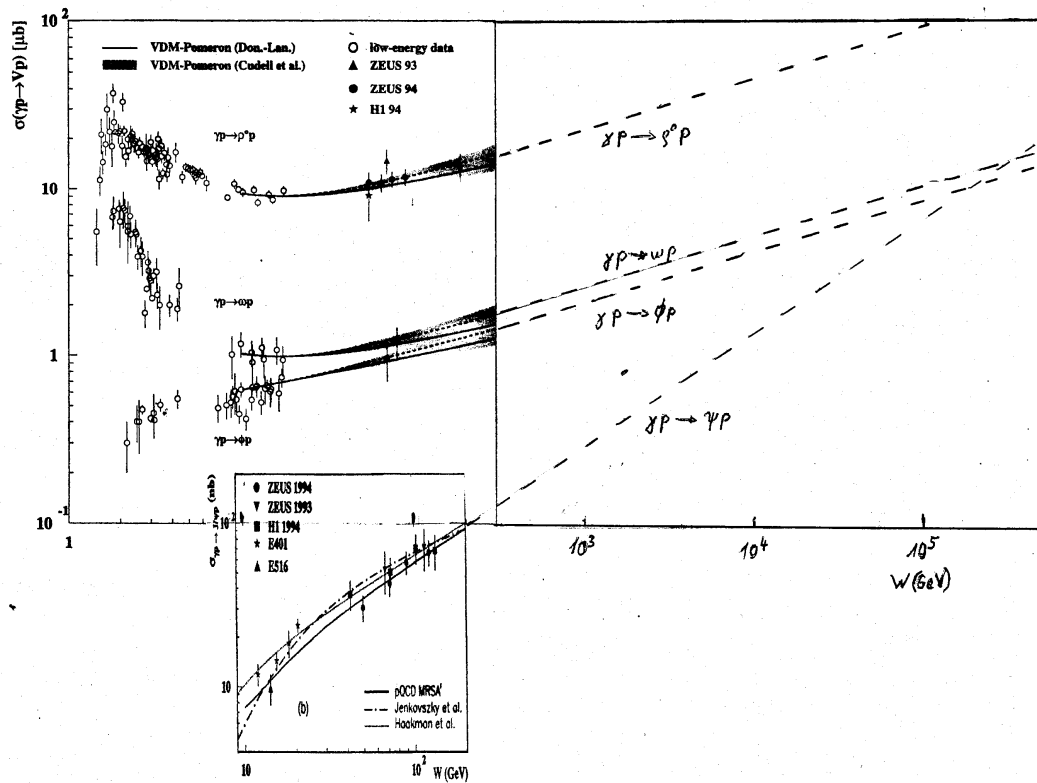


Figure 4: Experimental  $\gamma$ - $p$  cross-sections for different VMs, rescaled into one figure from Fig. 109 and Fig. 111 of Ref. [14]. Included are tentative extrapolations (dashed lines) to higher energies.

$$\sigma_{\rho^0} : \sigma_{\omega} : \sigma_{\phi} : \sigma_{\psi} = 9 : 1 : 2 : 8 \quad . \quad (5)$$

The greater the masses of the quark constituents of the  $\phi$ -meson, which consists essentially of a  $s\bar{s}$ -pair, and of the  $\psi$ -meson, which is formed by a  $c\bar{c}$ -pair, the more suppressed are their photoproduction probabilities thus modifying the ratios of Eq. 5. Experimental values for the production cross-section as function of energy are summarized in Fig. 4.

The  $\psi$ -meson has only a small decay branching ratio of  $\approx 6\%$  leading to a  $\mu^+\mu^-$ -pair (see Table 2). In all other modes muons may also be produced finally in the decay chains leading over charged pions, but in those cases the energy is distributed to much more particles thus reducing the occurrence of high-energy muons. The overall production of high-energy muons via a  $\psi$ -meson has to be compared with the direct production of a muon pair according  $\gamma \rightarrow \mu^+ + \mu^-$ , as described in Ref. [15].

With the tentative extrapolation of the  $\psi$ -production shown in Fig. 4 the muon production at  $E_{\text{cm}} = 10^4$  GeV is about a factor 10 less probable than the direct production via  $\gamma \rightarrow \mu^+ + \mu^-$ . At lower energies  $E_{\text{cm}} = 10^2$  GeV this factor reaches  $\approx 150$  and increases rapidly with decreasing energy because of the steep fall-off of the  $\psi$ -production cross-section, see Fig. 4. Therefore the production of  $\psi$ -mesons is neglected in CORSIKA.

In the present version of CORSIKA (7.350 issued Dec. 2012) also the  $\phi$ -meson production is not considered. Its cross-section is about 20 % below that of the  $\omega$ -meson. Despite its low decay branching ratio leading to  $K$ -mesons – the charged Kaons (produced in about the half of the  $\phi$ -decays) lead with 63.5 % to a muon, while only 27.1 % of the long living neutral Kaons decay directly to a muon – the short lifetime of the  $K$ -mesons (relative to that of the charged pions) favours the production of high-energy muons. Therefore it seems worth to consider the production of  $\phi$ -mesons in future versions of the CORSIKA program.

## References

- [1] G. Grammer, Jr. and D. Sullivan, in: *Electromagnetic Interactions of Hadrons*, ed. A. Donnachie and G. Shaw (Plenum Press, New York, 1978) Vol. **2**, 195
- [2] D. Schildknecht, *Acta Phys. Polon.* **B 37** (2006) 595; D. Schildknecht, G.A. Schuler, and B. Surrow, *Phys. Lett.* **B 449** (1999) 328
- [3] D. Heck et al., Report **FZKA 6019** (1998), Forschungszentrum Karlsruhe, available from: [http://www-ik.fzk.de/corsika/physics\\_description/corsika\\_phys.html](http://www-ik.fzk.de/corsika/physics_description/corsika_phys.html)
- [4] W.R. Nelson, H. Hirayama, and D.W.O. Rogers, Report **SLAC 265** (1985), Stanford Linear Accelerator Center; <http://www.slac.stanford.edu/pubs/slacreports/slacr-265.html>; [http://www.irs.inms.nrc.ca/inms/irs/EGS4/get\\_egs4.html](http://www.irs.inms.nrc.ca/inms/irs/EGS4/get_egs4.html)
- [5] T. Stanev, T.K. Gaisser, and F. Halzen, *Phys. Rev.* **D 32** (1985) 1244
- [6] J.R. Cudell et al., *Phys. Rev.* **D 61** (2000) 034019; Erratum: *Phys. Rev.* **D 63** (2001) 059901
- [7] J. Beringer et al. (Particle Data Group), *Phys. Rev.* **D 86** (2012) 010001; <http://pdg.lbl.gov/index.html>
- [8] P. Joos, in: *Landolt-Börnstein, New Series, Group I: Nuclear and Particle Physics*, ed. H. Schopper (Springer, Berlin, 1973) Vol. **8**, 306
- [9] R. Engel, private communication (2001)
- [10] R. Engel, J. Ranft, and S. Roesler, *Phys. Rev.* **D 55** (1997) 6957
- [11] A. Mücke et al., *Comp. Phys. Comm.* **124** (2000) 290
- [12] M. Derrick et al. (ZEUS Collab.), *Z. Phys.* **C 69** (1995) 39
- [13] D.W.G.S. Leith, in: *Electromagnetic Interactions of Hadrons*, ed. A. Donnachie and G. Shaw (Plenum Press, New York, 1978) Vol. **1**, 345
- [14] H. Abramowicz and A.C. Caldwell, *Rev. Mod. Phys.* **71** (1999) 1275
- [15] D. Heck, Report **FZKA 7525** (2009), Forschungszentrum Karlsruhe, available from: <http://www-ik.fzk.de/~heck/publications/>

KIT Scientific Working Papers  
ISSN 2194-1629

[www.kit.edu](http://www.kit.edu)